ADVANCED MATERIALS TECHNOLOGIES
www.advmattechnol.de

Check for updates

High-Resolution Pixelated Light Emitting Diodes Based on Electrohydrodynamic Printing and Coffee-Ring-Free Quantum Dot Film

Hegeng Li, Yongqing Duan, Zhilong Shao, Guannan Zhang, Huayang Li, YongAn Huang, and Zhouping Yin**

Inkjet printing for preparing quantum dot light emitting diodes (QLEDs) has become increasingly attractive due to its large-area, low-cost fabrication features. However, the rather low resolution and coarse morphology induced by the printing and uneven evaporation of droplet restrict its further development. Herein, electrohydrodynamic (EHD) printing and mixed solvent method are employed to fabricate high-resolution pixelated QLEDs. By optimizing the mixed solvent ratio to weaken capillary flow, coffee-ring-free quantum dot (QD) films can be obtained. With the help of EHD printing process optimization and pixel defining layers introduction, high-resolution pixelated QLED with 306 pixels per in. is achieved, which can meet the requirements of manufacturing mobile phones. Finally, an inverted pixelated QLED with a low turn-on voltage of 3 V and a maximum luminance of 8533 cd m^{-2} is fabricated, demonstrating that the presented strategy has huge potential in high-resolution and high-quality QD display manufacturing.

1. Introduction

Recently, colloidal quantum dots (QDs) have shown great potential in display and lighting field due to their outstanding properties, including high color saturation, narrow emission peak, high luminescent efficiency, and tunable emission colors by varying the size of QDs.[1–4] Based on the development of material and fabrication technology, quantum dot light emitting diodes (QLEDs) display has gradually reached the level of commercial application. For example, Peng's group[5] reported that the external quantum efficiency (EQE) of red-QLEDs had achieved 20.5% by inserting an insulating layer between the QD layer and the oxide electron-transport layer. Qian's group[6] demonstrated red, green, and blue QLEDs that all achieved high EQE over 10%. However, how to achieve high-resolution, low-cost, and large-area fabrication of QLED device is still a huge challenge.

Different from organic light emitting diode (OLED) which can utilize thermal vapor deposition to realize high-resolution patterning,[7] QLEDs are much more suitable for solution processing. Spin-coating[5,8] is the most commonly used method in laboratory, but it cannot achieve pattern fabrication. Transfer printing[9,10] is capable of realizing high-resolution patterning, but the complicated process is not compatible with large area fabrication. Inkjet printing[11,12] is a mask-free, material-effective, and large-area compatible manufacturing technology, and it has been considered to be appropriate for large-scale production of QLED displays.[13–15] However, traditional inkjet printing only meets the demand of television display with pixel density of about 100 pixels per in. (PPI), rather than mobile phones which require high-resolution pixels over 300 PPI. For example, Peng's group[16] has manufactured a 2-in. full-color QLEDs display with pixel density of 120 PPI and a color gamut of 109% (NTSC 1931).

Electrohydrodynamic (EHD) printing[17–20] provides a perfect scheme for high-resolution pixelated QLEDs fabrication. It utilizes a high voltage between nozzle and substrate to pull the polarized solution out, thereby deforming the meniscus into a conical shape from whose vertex a fine jet is ejected. Electric field force has a greater ability to drive droplets compared to traditional inkjet printing, so it possesses unique merits of high resolution (50 nm) and compatibility with wide viscosity range of inks (1–10 000 cP). For example, Kim et al.[21] printed a QD dot matrix with diameter of ≈5 µm, and Duan et al.[22] employed high-viscosity piezoelectric polyvinylidine fluoride (PVDF) to prepare piezoelectric nanofiber array by electrospinning. To achieve high-resolution pixelated device, precise control of droplet volume and film morphology are essential to get rid of coffee-ring and mura defects, thus to improve the photoelectric performance of device. Printing a small volume of solution in the pixel pit multiple times can reduce the volume error, which can be achieved by high-resolution EHD printing. By adjusting the balance of capillary flow driven by concentration variation and maragoni flow caused by surface tension variation during

H. Li, Dr. Y. Q. Duan, Z. Shao, G. Zhang, H. Li, Prof. Y. A. Huang, Prof. Z. Yin
State Key Laboratory of Digital Manufacturing Equipment and Technology
Flexible Electronics Research Center
Huazhong University of Science and Technology
Wuhan 430074, China
E-mail: duanyongqing@hust.edu.cn; yinzhp@mail.hust.edu.cn

The ORCID identification number(s) for the author(s) of this article can be found under https://doi.org/10.1002/admt.202000401.

DOI: 10.1002/admt.202000401

 © 2020 WILEY-VCH Verlag GmbH & Co. KGaA, Weinheim

drop evaporation, coffee-ring phenomenon has been improved a lot. For example, Liu et al.[23] lowered the temperature of the substrate, Yunker et al.[24] changed the shape of the particles, Li et al.[25] increased the viscosity of perovskite solution, Liu et al.[13] and Jiang et al.[15] applied mixed solvent to balance the capillary flow and the maragoni flow to eliminate the coffee-ring phenomenon.

In this work, we combined high-resolution EHD printing technology and mixed solvent method to manufacture high-quality and high-resolution pixelated QLED device with perfect morphology of QD films. Two solvents, cyclohexylbenzene (CHB) and nonane, have been selected as the mixed solvent for QD ink, and the volume ratio of 8:2 is proved to be perfect. Through optimizing the EHD printing process, we can accurately control the volume of the droplet to realize controllable QD film thickness. Further, high-resolution pixelated QD films of 306 PPI and QD dot arrays with diameter of 1 µm can be attained. Finally, based on the perfect film printed, we prepared an inverted pixelated QLED device of which EQE and maximum luminance can achieve 0.55% and 8533 cd m^{-2}, respectively. The results lay a solid foundation for manufacture of high-resolution displays.

2. Results and Discussion

A bottom-emitting pixelated device with inverted structure[26,27] has been demonstrated in **Figure 1**a, consisting of ITO/ZnO/Red-QD/NPB/MoO_3/Al layers. QDs, ITO, and Al are adopted as light emitting layer, cathodes, and anodes, respectively. ZnO, NPB, and MoO_3 are chosen as the electron transport layer, hole transport layer, and hole injection layer to match the energy levels as shown in Figure 1b, where NPB/MoO_3 make use of the deep highest occupied molecular orbit energy level to realize efficient hole injection into the QD layer, and ZnO achieves efficient electron injection into QD layer considering its high electron mobility. Meanwhile, pixel definition layers (PDL) with good insulativity are designed where a luminescent layer and multi-functional layers will be deposited inside in sequence, to avoid the short circuit of devices. And EHD printing has been introduced to fill the pixelated substrate and realize high-resolution patterning of the emitting layer as shown in Figure 1c.

To control the morphology of QD films, CHB with high boiling point is chosen as the main solvent, nonane with low surface tension/viscosity and low toxicity is mixed with CHB to solve the coffee-ring problem, considering that it is much more suitable for EHD printing for requiring lower driving force and it is less harm to human body. A series of QD inks with different solvent ratio under a UV light are shown in Figure 1d. Furthermore, the top of Figure 1e demonstrates the direction of the capillary flow and Maragoni flow inside the droplet. By regulating the two microscopic behaviors, coffee-ring film (Figure 1e middle) and coffee-ring-free film (Figure 1e bottom) can be obtained.

Figure 2 shows the various morphology of the QD dot arrays on ZnO layer with different volume ratios of CHB containing 100%, 90%, 80%, 70%, and 0%. Figure 2a and its enlarged view Figure 2b demonstrate fluorescent microphotographs of printed dots. Figure 2c,d shows the 3D and 2D image of the white light interferometer of a single dot. From the fluorescent picture, we can see that the QD films exhibit serious coffee-ring and can only emit heterogeneous light when only CHB is used as the solvent. With the increase of nonane, the coffee-ring is gradually suppressed and completely disappeared when the mixed solvent ratio is 8:2. With further increase of nonane, the coffee-ring appears again and the QD film emit uneven light. As the ratio reaches 0:10, only the edge part can emit weak light. From the 3D morphology pictures and 2D sectional view of the QD single dot, it can be seen that the middle and edge of the film are slightly high when CHB is used as the single solvent. When nonane is added, most of the film is flat, but the edge part is much higher than the flat part. A flat film can be obtained as the volume ratio of the two solvents reaches 8:2. However, when the ratio of nonane continues to increase, the thickness difference between the film edge and the film center becomes larger, which means that the coffee-ring is worse. The result of the fluorescent picture is consistent with morphology measurement of the white light interferometer.

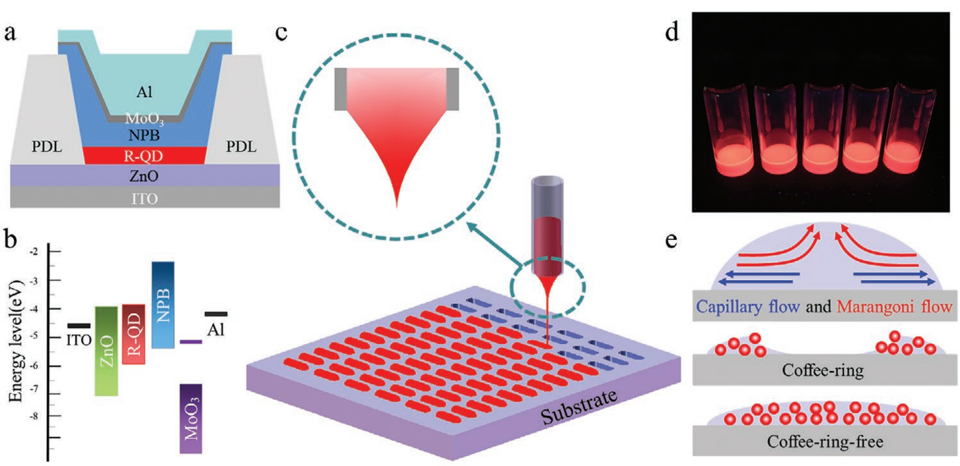

Figure 1. a) Structure diagram of the QLED device. b) Energy level diagram of the QLED. c) Schematic of EHD printing to fill the pixel. d) Image of QD inks with different solvent volume ratios, CHB:nonane is 10:0, 9:1, 8:2, 7:3, 0:10 from left to right respectively. e) Schematic diagram of film morphology with or without coffee-ring.

© 2020 WILEY-VCH Verlag GmbH & Co. KGaA, Weinheim

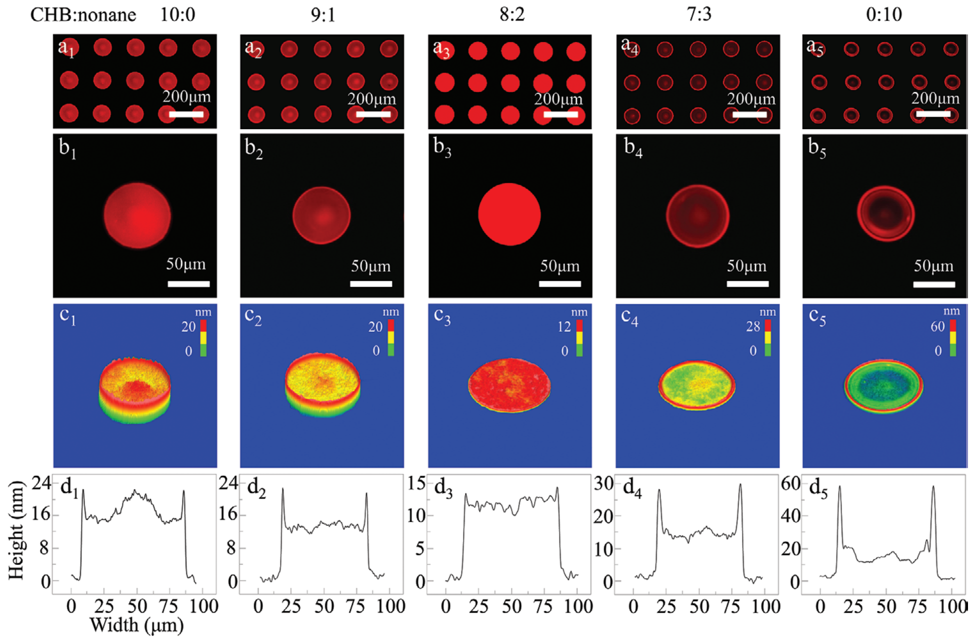

Figure 2. a1–a5) Fluorescent microphotographs of QD dot arrays on ZnO layer printed with different inks. b1–b5) Higher resolution fluorescent microphotographs of a single dot according to (a1–a5). c1–c5) 3D morphology images of the white light interferometer. d1–d5) The film thickness profile of each single dot.

In order to explain the above phenomenon, solution properties including surface tension and viscosity are measured (**Table 1**). The viscosity and surface tension of CHB are 2.81 cP and 27.2 mN m^{-1}, respectively, both higher than the viscosity (0.72 cP) and surface tension (22.8 mN m^{-1}) of nonane. Single solvent solution is difficult to get flat film because the concentration difference caused by the uneven evaporation will guide the solution to flow from center to edge.[28] Therefore, ink 1 and ink 5 both have coffee-ring phenomenon. As for the mixed solvent solution, the addition of nonane decreases the viscosity of QD inks from 2.29 to 1.69 cP (ink 2 to ink 4). However, the surface tension reaches a maximum value when the volume ratio of the two solvents is 8:2, this may be caused by a small amount of QD dissolved in nonane, which has a higher surface tension than that of pure nonane[15] but the solubility of QDs is limited.

We know that as the viscosity increases, the capillary flow of the solution weakens and the coffee-ring phenomenon is limited. Meanwhile, according to Young's equation:

$$\cos\theta = \frac{\gamma_{sg} - \gamma_{sl}}{\gamma_{lg}} \quad (1)$$

where γ_{sg}, γ_{sl}, γ_{lg} represent solid–gas surface tension, solid–liquid surface tension, and liquid–gas surface tension, respectively. γ_{lg} is equivalent to surface tension of solution. From the equation, when γ_{sg} and γ_{sl} remain constant, the surface tension of the solution is proportional to the contact angle. According to previous studies,[13] as the contact angle increases, the capillary flow weakens and the coffee-ring is inhibited. Therefore, a perfect film can be obtained with the help of viscosity and surface tension when the volume ratio is 8:2. The spectrum and absorption curve of ink 3 are shown in Figure S1, Supporting Information, where the luminous peak at 632 nm and a full width at half maximum of 32 nm are consistent with the properties of QD powder.

Table 1. Viscosity and surface tension of QD solutions with different solvent ratios.

Ink	1	2	3	4	5
CHB/nonane	10:0	9:1	8:2	7:3	0:10
Viscosity [cP]	2.81	2.29	1.96	1.69	0.72
Surface tension [mN m^{-1}]	27.2	23.8	24.2	23.7	22.8

In order to achieve precise control of the droplet volume in the pixel pit, it is necessary to study the effect of voltage process parameters on the volume of the droplet. According to previous research,[29,30] the cone-jet state is the most suitable mode to achieve high-resolution patterning. As demonstrated in **Figure 3**a, a cone-jet mode rather than multi-jet mode will be obtained when the process parameters are within an appropriate range, which can print high-resolution droplets in a stable state. And the influence of peak voltage, duty ratio, and frequency of pulse voltage (defined in Figure S2a, Supporting Information) on the droplet volume in cone-jet mode have been carefully studied. Figure 3b,c demonstrates that the droplet diameter increases approximately linearly with peak voltage and duty cycle in the range of 680–920 V and 5–14% respectively, while is inversely proportional to the pulse frequency from 10 to 80 Hz (Figure 3d). Meanwhile, Figure 3e proves that the drop generation frequency is equal to pulse frequency, and it supports high frequency printing (i.e., 1000 Hz), which is essential for commercial application.

Based on the printing rules above and using a small nozzle with 5 μm diameter, a high-resolution QD matrix with diameters of 1 μm can be obtained as shown in **Figure 4**a,

© 2020 WILEY-VCH Verlag GmbH & Co. KGaA, Weinheim

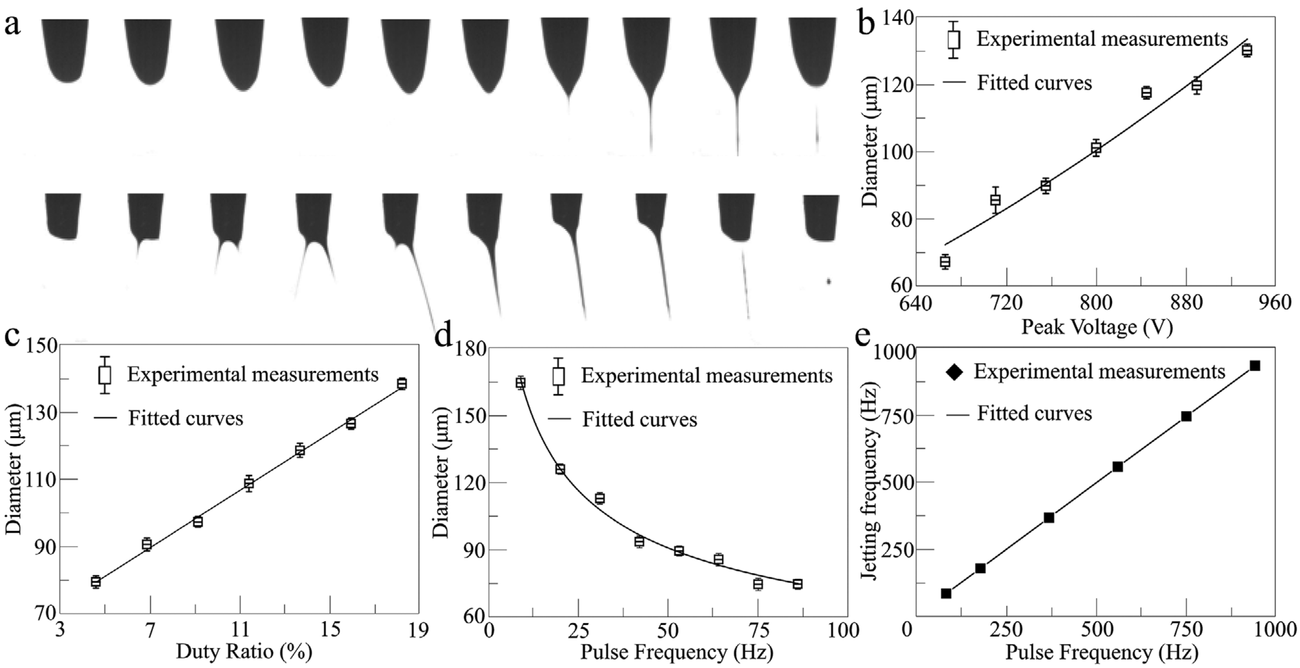

Figure 3. a) High-speed camera images of EHD jet with a steady cone-jet or unsteady multi-jet. b) QD dot diameter versus pulse peak voltage. c) QD dot diameter versus pulse duty ratio. d) QD dot diameter versus pulse frequency. e) Jetting frequency versus pulse frequency.

demonstrating that EHD printing has superior advantage in preparation high-resolution displays. The specific printing parameters including high-resolution array and pixelated patterns can be found in Table S1, Supporting Information.

With regard to display applications, it is necessary to deposit QD inks in high-resolution pixel pits. First, PDL with outstanding hydrophobicity is prepared by photolithography to ensure that the QD ink in each pit does not contaminate. The contact angle of the QD solution on the photoresist and ZnO layer is 63.19° and less than 8° (Figure S3, Supporting Information) respectively, and pixelated substrates with different resolutions can be obtained as shown in Figure S4, Supporting Information. Next, EHD printing was applied to print QD ink into pixel pit. The black pixel pit in the left of Figure 4b is filled with QD ink and the

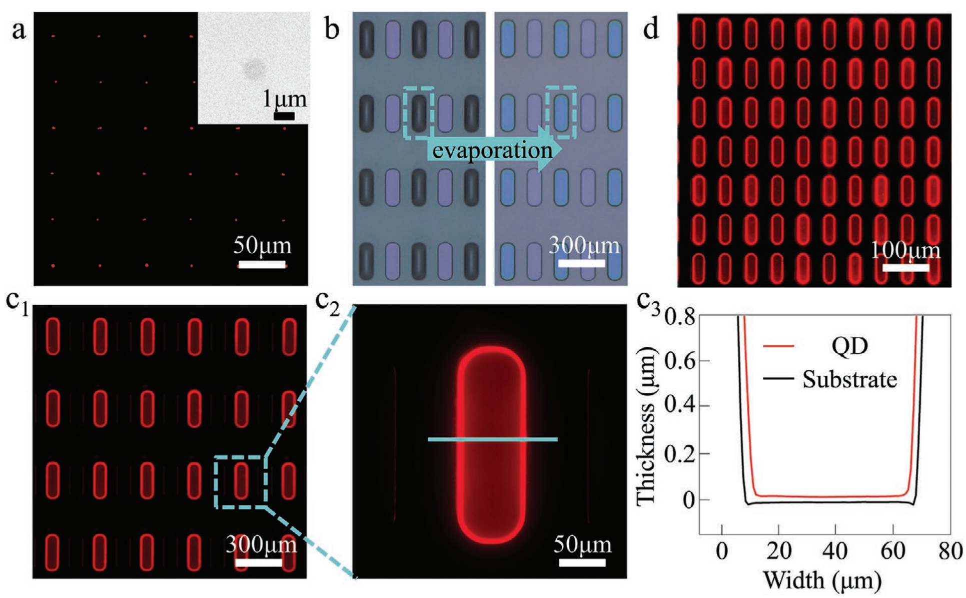

Figure 4. a) The fluorescent image of high-resolution QD arrays and the scanning electron microscopy (SEM) image of a high-resolution dot with diameter of 1 μm. b) The optical picture of the QD layer before and after drying. c_1,c_2) The fluorescent microphotographs and enlarged fluorescent image of pixels with 73 PPI. c_3) The film thickness profile of a single pixel pit. d) The fluorescent microphotograph of high-resolution pixels with 306 PPI.

© 2020 WILEY-VCH Verlag GmbH & Co. KGaA, Weinheim

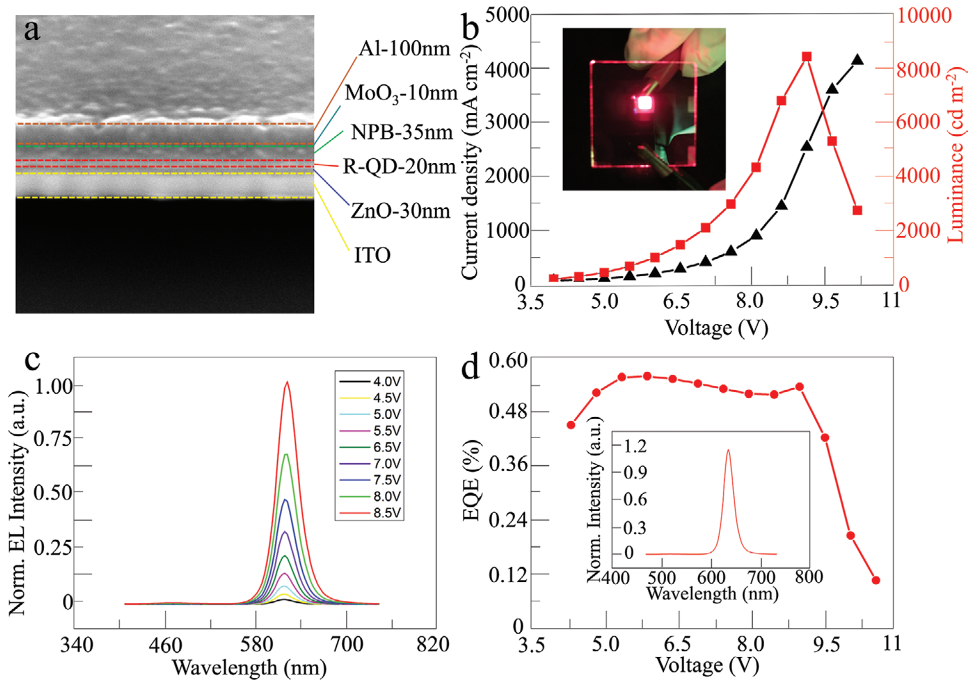

Figure 5. a) Cross-sectional SEM image of QLED device. b) *J–V–L* characteristics of QLED. c) Luminance of QLED device under different voltages. d) The dependence of EQE on the voltage and the electroluminescence (EL) spectra of QLED.

right of Figure 4b demonstrates the optical photo of QD film after vacuum drying. The pixel pit size of 73 PPI is 60 µm × 175 µm and we print 7 drops per pixel pit with a spacing of 20 µm between each drop, to meet the volume demand and reduce the total volume error compared to 1 big drop. Figure 4c_1,c_2 demonstrates the QD film in the pixel pit of 73 PPI is very uniform, and the pixel edge is brighter than the middle because the edge has a certain inclination angle which induces light accumulation. Further, the white light interferometer were used to characterize the thickness and uniformity of the QD film in the pixel pit in Figure 4c_3, proving that the printed QD film is of good quality. Finally, high-resolution QD pixels of 306 PPI (20 µm × 60 µm) has been fabricated as shown in Figure 4d.

An inverted pixelated QLED has been fabricated and characterized in **Figure 5**. Inverted structure is chosen here considering that it is more compatible with mature n-type organic thin film transistor in actual industrialization. The specific manufacturing sequence is: magnetron sputtering to prepare ZnO, EHD printing to obtain QD layer, and thermal evaporation to deposit NPB, MoO_3, and Al. In order to protect ZnO layer from been destroyed by QD solvent, magnetron sputtering is applied to ensure that ZnO is dense and strong. The cross-sectional image of the device in Figure 5a demonstrates that each layer has very clear interface, and no mutual dissolution exists. Figure 5b shows the *J–V–L* characteristics. The QLED exhibits a low turn-on voltage (applied voltage when luminance is 1 cd m^{-2}) of about 3 V and a maximum luminance of 8533 cd m^{-2} at 9 V. The QD device at a bias of 7 V (Figure 5b) exhibits excellent emission homogeneity without any dead pixels. Figure 5c tests the spectrum of the device under different voltages, proving that the emission spectrum of the device does not shift at any voltage, and the peak value at 632 nm is consistent with QD solution. The EQE of the device is a core indicator to evaluate its photoelectric conversion performance. Figure 5d shows the peak EQE is 0.55%, which is at the same level of existing low-resolution pixelated devices fabricated by inkjet printing,[13] which is of great significance for manufacturing high-resolution QD display.

3. Conclusion

In conclusion, this paper combined powerful EHD printing and mixed solvent method to realize high-resolution and high-quality pixelated QLED fabrication. Experiments and theoretical analysis have demonstrated the coffee-ring is completely suppressed when the mixed solvent ratio of CHB:nonane is 8:2. By precise control of the droplet volume through printing parameters modification, high-resolution QD dot matrix with diameter of 1 µm and pixel pits at 306 PPI have been successfully fabricated. Based on the perfect QD film in each pixel pit, inversed pixelated QLEDs that have a low turn on voltage of 3 V and a maximum luminance of 8533 cd m^{-2} at the voltage of 9 V are fabricated. This achievement of high-resolution and high brightness QLED device demonstrates their great potential in commercial QD display manufacturing.

4. Experimental Section

Materials: Red (CdSe/CdS/ZnS) QD powders were purchased from Guangdong Poly OptoElectronics Co. Ltd. *N*,*N*′-di(1-naphthyl)-*N*,*N*′-diphenyl-(1,1′-biphenyl)-4,4′-diamine (NPB) and molybdenum trioxide (MoO_3) were purchased from Aladdin Co. Ltd. Nonane and CHB with purity higher than 99% were purchased from Sigma Co. Ltd. Aluminum (Al) and ZnO target were purchased from Zhongnuoxincai Co. Ltd. Photoresist was purchased from Futurrex Co. Ltd., USA.

 © 2020 WILEY-VCH Verlag GmbH & Co. KGaA, Weinheim

Fabrication of QLEDs: Pixelated QLED devices were fabricated in the following procedure. ITO-coated glass substrates were cleaned by ultrasonication in acetone, isopropyl alcohol, and deionized water successively. The substrates were dried by using flowing nitrogen gas. ZnO layer was prepared on ITO by magnetron sputtering with a power of 100 W and a ratio of oxygen to argon of 29:1. The substrates were irradiated by UV/oxygen plasma for 20 min to increase hydrophilicity of the substrate surface, and then photoresist was spin-coated, followed by lithography to obtain pixel pits with different resolutions. A high-resolution EHD printer (EHDJet-P professional type, Guangdong Sygole Intelligent Technology Co. Ltd.) was used to print QD solutions into the pixels. After printing, the substrate was baked on a hot plate at 80 °C for 10 min. All of the solution processes were carried out in ambient environment. Finally, the substrates were transferred to a vacuum chamber below 3×10^{-4} Pa to deposit NPB, MoO_3, and Al anode in sequence.

Characterization: The surface tension and viscosity of QD inks were measured by surface tension meter (KRUSS, K20) and Brookfield Rotational Viscometer (DV3TLVCJ0) at room temperature, respectively. The emission spectrum was measured by HORIBA JY FluoroMax-4 fluorescence spectrophotometer. UV–vis spectrophotometer (PerkinElmer instruments, Lambda 950 using integrating sphere) was applied to study the optical absorption of QD inks. The 3D images of dot microarrays were characterized by White light interferometer (ZYGO, NewView 7100). A fluorescent microscope (Nikon eclipse Ts2R) characterized the photoluminescence (PL) images of the microarrays. The optic images of the pixel were obtained by light microscope (Olympus, DSX510). The jetting process was visualized by a high-speed camera (Dimax HD, PCO AG) with a zoom lens (magnification 1.16–13.92, Navitar Inc.). The surface of microarray and sectional view of device were measured by field emission scanning electron microscopy (FE-SEM, FEI NOVA NanoSEM 450). Magnetron sputtering and thermal evaporation that both come from SKY Technology Development could manufacture functional layers and electrode. Lithography machine (ABM/6/350/NUUV/DCCD/BSV/M) could manufacture pixel pit. Voltage–luminance–current curves were measured by a system containing Photo Research's PR-655 and a Keithley 4200 source list.

Supporting Information

Supporting Information is available from the Wiley Online Library or from the author.

Acknowledgements

This work was financially supported by the National Key Research and Development Program of China (2018YFA0703200), the National Natural Science Foundation of China (51605180, 51705181, and 51925503). The authors would also like to thank Flexible Electronics Manufacturing Laboratory in Comprehensive Experiment Center for advanced manufacturing and equipment technology.

Conflict of Interest

The authors declare no conflict of interest.

Keywords

coffee-ring, electrohydrodynamic printing, mixed solvent, pixel defining layers, QLEDs

Received: April 26, 2020
Revised: June 15, 2020
Published online:

[1] X. Dai, Y. Deng, X. Peng, Y. Jin, *Adv. Mater.* **2017**, *29*, 1607022.
[2] L. Qian, Y. Zheng, J. Xue, P. H. Holloway, *Nat. Photonics* **2011**, *5*, 543.
[3] L. Xie, X. Xiong, Q. Chang, X. Chen, C. Wei, X. Li, M. Zhang, W. Su, Z. Cui, *Small* **2019**, *15*, 1900111.
[4] M. Zhang, B. Hu, L. Meng, R. Bian, S. Wang, Y. Wang, H. Liu, L. Jiang, *J. Am. Chem. Soc.* **2018**, *140*, 8690.
[5] X. Dai, Z. Zhang, Y. Jin, Y. Niu, H. Cao, X. Liang, L. Chen, J. Wang, X. Peng, *Nature* **2014**, *515*, 96.
[6] Y. Yang, Y. Zheng, W. Cao, A. Titov, J. Hyvonen, J. R. Manders, J. Xue, P. H. Holloway, L. Qian, *Nat. Photonics* **2015**, *9*, 259.
[7] X. Ai, E. W. Evans, S. Dong, A. J. Gillett, H. Guo, Y. Chen, T. J. H. Hele, R. H. Friend, F. Li, *Nature* **2018**, *563*, 536.
[8] Y. Liu, C. Jiang, C. Song, J. Wang, L. Mu, Z. He, Z. Zhong, Y. Cun, C. Mai, J. Wang, J. Peng, Y. Cao, *ACS Nano* **2018**, *12*, 1564.
[9] M. K. Choi, J. Yang, K. Kang, D. C. Kim, C. Choi, C. Park, S. J. Kim, S. I. Chae, T. H. Kim, J. H. Kim, T. Hyeon, D. H. Kim, *Nat. Commun.* **2015**, *6*, 7149.
[10] T. H. Kim, K. S. Cho, E. K. Lee, S. J. Lee, J. Chae, J. W. Kim, D. H. Kim, J. Y. Kwon, G. Amaratunga, S. Y. Lee, B. L. Choi, Y. Kuk, J. M. Kim, K. Kim, *Nat. Photonics* **2011**, *5*, 176.
[11] M. Duan, Z. Feng, Y. Wu, Y. Yin, Z. Hu, W. Peng, D. Li, S.-j. Chen, C.-Y. Lee, A. Lien, *Adv. Mater. Technol.* **2019**, *4*, 1900779.
[12] Z. Gu, K. Wang, H. Li, M. Gao, L. Li, M. Kuang, Y. S. Zhao, M. Li, Y. Song, *Small* **2017**, *13*, 1603217.
[13] Y. Liu, F. Li, Z. Xu, C. Zheng, T. Guo, X. Xie, L. Qian, D. Fu, X. Yan, *ACS Appl. Mater. Interfaces* **2017**, *9*, 25506.
[14] X. Xiong, C. Wei, L. Xie, M. Chen, P. Tang, W. Shen, Z. Deng, X. Li, Y. Duan, W. Su, H. Zeng, Z. Cui, *Org. Electron.* **2019**, *73*, 247.
[15] C. Jiang, Z. Zhong, B. Liu, Z. He, J. Zou, L. Wang, J. Wang, J. Peng, Y. Cao, *ACS Appl. Mater. Interfaces* **2016**, *8*, 26162.
[16] C. Jiang, L. Mu, J. Zou, Z. He, Z. Zhong, L. Wang, M. Xu, J. Wang, J. Peng, Y. Cao, *Sci. China: Chem.* **2017**, *60*, 1349.
[17] J. U. Park, M. Hardy, S. J. Kang, K. Barton, K. Adair, D. K. Mukhopadhyay, C. Y. Lee, M. S. Strano, A. G. Alleyne, J. G. Georgiadis, P. M. Ferreira, J. A. Rogers, *Nat. Mater.* **2007**, *6*, 782.
[18] J. Liu, L. Xiao, Z. Rao, B. Dong, Z. Yin, Y. A. Huang, *Adv. Mater. Technol.* **2018**, *3*, 1800155.
[19] M. S. Onses, E. Sutanto, P. M. Ferreira, A. G. Alleyne, J. A. Rogers, *Small* **2015**, *11*, 4237.
[20] Y. Jiang, C. Wu, L. Li, K. Wang, Z. Tao, F. Gao, W. Cheng, J. Cheng, X. Y. Zhao, S. Priya, W. Deng, *Nano Energy* **2018**, *53*, 440.
[21] B. H. Kim, M. S. Onses, J. Bin Lim, S. Nam, N. Oh, H. Kim, K. J. Yu, J. W. Lee, J. H. Kim, S. K. Kang, C. H. Lee, J. Lee, J. H. Shin, N. H. Kim, C. Leal, M. Shim, J. A. Rogers, *Nano Lett.* **2015**, *15*, 969.
[22] Y. Duan, Y. Huang, Z. Yin, N. Bu, W. Dong, *Nanoscale* **2014**, *6*, 3289.
[23] Y. Liu, F. Li, L. Qiu, K. Yang, Q. Li, X. Zheng, H. Hu, T. Guo, C. Wu, T. W. Kim, *ACS Nano* **2019**, *13*, 2042.
[24] P. J. Yunker, T. Still, M. A. Lohr, A. G. Yodh, *Nature* **2011**, *476*, 308.
[25] H. Li, N. Liu, Z. Shao, H. Li, L. Xiao, J. Bian, J. Li, Z. Tan, M. Zhu, Y. Duan, L. Gao, G. Niu, J. Tang, Y. Huang, Z. Yin, *J. Mater. Chem. C* **2019**, *7*, 14867.
[26] H. Zhang, H. Li, X. Sun, S. Chen, *ACS Appl. Mater. Interfaces* **2016**, *8*, 5493.
[27] C. Jiang, H. Liu, B. Liu, Z. Zhong, J. Zou, J. Wang, L. Wang, J. Peng, Y. Cao, *Org. Electron.* **2016**, *31*, 82.
[28] R. D. Deegan, O. Bakajin, T. F. Dupont, *Nature* **1997**, *389*, 827.
[29] J. Kim, H. Oh, S. S. Kim, *J. Aerosol Sci.* **2008**, *39*, 819.
[30] K. Barton, S. Mishra, A. Alleyne, P. Ferreira, J. Rogers, *Control Eng. Pract.* **2011**, *19*, 1266.

© 2020 WILEY-VCH Verlag GmbH & Co. KGaA, Weinheim